Electromagnetic analysis of cylindrical cloaks of an arbitrary cross section

André Nicolet,[1] Frédéric Zolla,[1] and Sébastien Guenneau[2,*]

[1] *Institut Fresnel, UMR CNRS 6133, University of Aix-Marseille, Case 162, F13397 Marseille Cedex 20, France*
[2] *Department of Mathematical Sciences, University of Liverpool, Peach Street, Liverpool L693BX, UK*
**Corresponding author: guenneau@liverpool.ac.uk*

Received April 22, 2008; accepted May 26, 2008;
posted June 10, 2008 (Doc. ID 95342); published July 11, 2008

We extend the design of radially symmetric invisibility cloaks through transformation optics as proposed by Pendry *et al.* [Science **312**, 1780 (2006)] to coated cylinders of an arbitrary cross section. The validity of our Fourier-based approach is confirmed by both analytical and numerical results for a cloak displaying a nonconvex cross section of varying thickness. In the former case, we evaluate the Green's function of a line source in the transformed coordinates. In the latter case, we implement a full-wave finite-element model for a cylindrical antenna radiating a p-polarized electric field in the presence of a F-shaped lossy object surrounded by the cloak. © 2008 Optical Society of America

OCIS codes: 110.4190, 220.3630, 260.2110.

Metamaterials (known for their subwavelength imaging applications [1–3]) open new avenues in electromagnetic cloaking, either through their heterogeneous anisotropic effective material parameters (transformation optics [4,5]) or through low-index materials [6] or negative refractive index materials [7]. Interestingly, the invisibility is preserved in the case of an intense near field [8], when the ray optics picture breaks down. Nevertheless, the first experimental realization, chiefly achieved in the microwave regime [9], suggests that cloaking will be limited to a very narrow range of frequencies. In the optical spectrum, it will be also necessarily dissipative and dispersive [10].

In the present Letter, we discuss the design of cylindrical cloaks with an arbitrary cross section described by two functions, $R_1(\theta)$ and $R_2(\theta)$, giving an angle-dependent distance from the origin. These functions correspond respectively to the interior and exterior boundary of the cloak. We shall only assume that these two boundaries can be represented by a differentiable function described, e.g., by a finite Fourier expansion. Hence, our approach can be applied not only to elliptic cloaks [11,12] but also to cloaks with smooth nonconvex boundaries (but not square shaped [13]).

To illustrate our methodology, we consider a cloak that does not possess any rotational or translational symmetry in the transverse plane. We first inspect the cloak parameters at its nonreflecting outer boundary (see Fig. 1). We then compute the full-wave picture (via finite elements) for a lossy object with sharp wedges surrounded by the cloak in presence of a closely located antenna (see Figs. 2 and 3). We finally compare these numerical results against an analytical model by evaluating the Green's function of a p-polarized electric line source in the corresponding transformed metric (see Fig. 4). This confirms that cloaking holds not only for the far field but also for the near field, where the ray model of the field breaks down.

The geometric transformation that maps the field within the full domain $\rho \leqslant R_2(\theta)$ onto the annular domain $R_1(\theta) \leqslant \rho' \leqslant R_2(\theta)$ can be expressed as

$$\begin{cases} \rho'(\rho,\theta) = R_1(\theta) + \rho \dfrac{R_2(\theta) - R_1(\theta)}{R_2(\theta)} \\ \theta' = \theta, \quad 0 < \theta \leqslant 2\pi \\ z' = z, \quad z \in \mathbb{R} \end{cases}, \tag{1}$$

where $0 \leqslant \rho \leqslant R_2(\theta)$. Note that the transformation maps the field for $\rho > R_2(\theta)$ onto itself through the identity transformation.

This change of coordinates is characterized by the transformation of the differentials through the Jacobian:

$$\mathbf{J}(\rho',\theta') = \frac{\partial(\rho(\rho',\theta'),\theta,z)}{\partial(\rho',\theta',z')}. \tag{2}$$

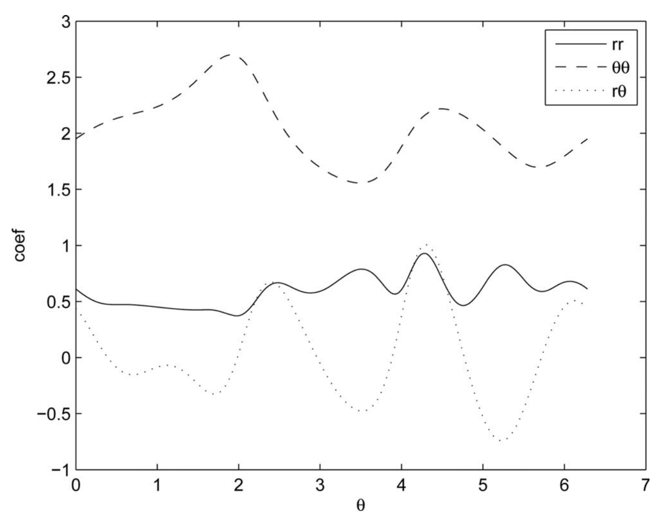

Fig. 1. Variation of entries $(T^{-1})_{rr}$, $(T^{-1})_{r\theta}=(T^{-1})_{\theta r}$, and $(T^{-1})_{\theta\theta}=(T^{-1})_{zz}=c_{11}$ of the inverse metric tensor $\mathbf{T}^{-1}$ on the outer boundary $R_2(\theta)$ of the cloak with respect to the angle θ in radians [c.f. Eqs. (4) and (6)].

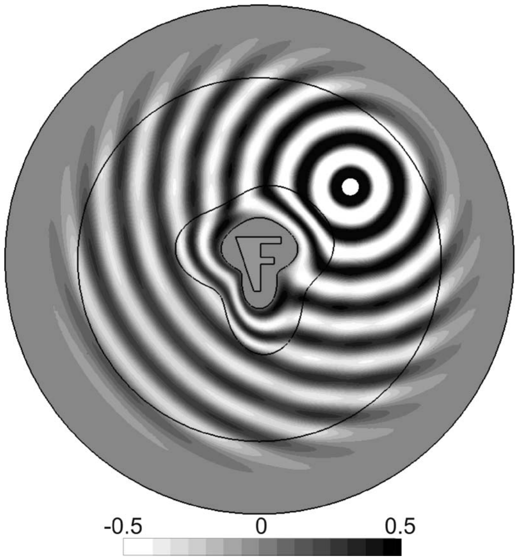

Fig. 2. Real part of the longitudinal electric field E_z radiated by a wire source antenna centered at point (2.5,2) in presence of the arbitrary cloak with boundaries defined by Eq. (9). The central computational domain is a disk centered at point (0,0) of radius 4. It is surrounded by an annulus of perfectly matched layers ($4 \leqslant \rho \leqslant 5$).

From an electromagnetic point of view, this change of coordinates amounts to mapping a homogeneous isotropic medium with scalar permittivity and permeability ϵ and μ, onto a material described by anisotropic heterogeneous matrices of permittivity and permeability given by [8,14]

$$\underline{\underline{\epsilon}}' = \epsilon \mathbf{T}^{-1}, \qquad \underline{\underline{\mu}}' = \mu \mathbf{T}^{-1}, \tag{3}$$

where $\mathbf{T} = \mathbf{J}^T \mathbf{J} / \det(\mathbf{J})$ is a representation of the metric tensor in the so-called stretched radial coordinates.

After some elementary algebra, we find that

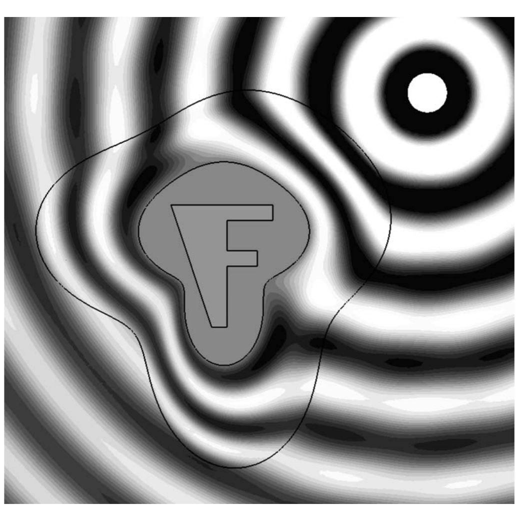

Fig. 3. Zoom on the central region of Fig. 2.

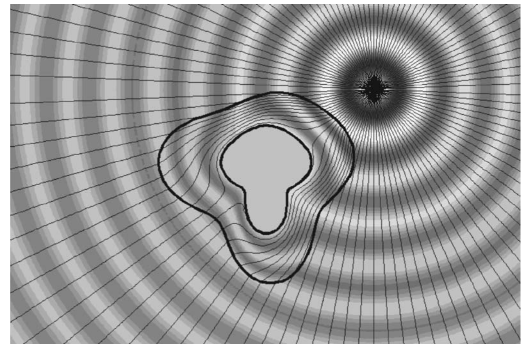

Fig. 4. Green's function in transformed coordinates and associated ray picture. Boundaries of the corresponding cloak are drawn for comparison with Figs. 2 and 3.

$$\mathbf{T}^{-1} = \begin{pmatrix} \dfrac{c_{12}^2 + f_\rho^2}{c_{11} f_\rho \rho'} & -\dfrac{c_{12}}{f_\rho} & 0 \\ -\dfrac{c_{12}}{f_\rho} & \dfrac{c_{11}\rho'}{f_\rho} & 0 \\ 0 & 0 & \dfrac{c_{11} f_\rho}{\rho'} \end{pmatrix}, \tag{4}$$

where $c_{11}(\theta') = R_2(\theta')/[R_2(\theta') - R_1(\theta')]$ and

$$c_{12}(\rho', \theta') = [\rho' - R_2(\theta')] R_2(\theta') \frac{\mathrm{d}R_1(\theta')}{\mathrm{d}\theta'} - \frac{[\rho' - R_1(\theta')] R_1(\theta')}{[R_2(\theta') - R_1(\theta')]^2} \frac{\mathrm{d}R_2(\theta')}{\mathrm{d}\theta'}, \tag{5}$$

for $R_1(\theta') \leqslant \rho' \leqslant R_2(\theta')$, with

$$f_\rho(\rho', \theta') = [\rho' - R_1(\theta')] \frac{R_2(\theta')}{R_2(\theta') - R_1(\theta')}. \tag{6}$$

Elsewhere, $\mathbf{T}^{-1}$ reduces to the identity matrix [$c_{11} = 1$, $c_{12} = 0$, and $f_\rho = \rho'$ for $\rho' > R_2(\theta')$].

We would like now to look at the electromagnetic field radiated by a wire source antenna centered at point $\mathbf{r}_s$ in presence of a finite conducting object shaped as a letter "F" when it is surrounded by an arbitrarily shaped cloak. Thanks to the cylindrical geometry, the problem splits into two polarizations. In p polarization, we find

$$\nabla(\underline{\underline{\mu}}_T'^{-1} \nabla E_z) + \mu_0 \epsilon_0 \omega^2 \epsilon_{zz}' E_z = -i\omega I_s \mu_0 \delta_{\mathbf{r}_s}, \tag{7}$$

where $\mu_0 \epsilon_0 = c^{-2}$, c being the speed of light in vacuum, $\underline{\underline{\mu}}_T'^{-1}$ stands for the upper bloc diagonal part of $\underline{\underline{\mu}}'^{-1}$ [see Eqs. (3) and (4)], and $\epsilon_{zz}' = \epsilon(c_{11} f_\rho / \rho')$. Also, E_z and I_s stand respectively for the only nonzero components of the longitudinal electric field $\mathbf{E}_l = E_z(\rho, \theta)\mathbf{e}_z$, and a given electric current $\mathbf{J}_s = I_s \delta_{\mathbf{r}_s} \mathbf{e}_z$ on the wire antenna.

The weak form of this equation has been implemented in the finite-element freeware GetDP [15], where circular perfectly matched layers were used to model the infinite outer medium surrounding the cloak. We first looked at a cylindrical cloak of elliptical cross section parameterized as $\rho(\theta) = ab/\sqrt{a^2\cos(\theta)^2+b^2\sin(\theta)^2}$. We checked that it provides exactly the same wave trajectories and field profile as in [12], where similar results were obtained through a space dilatation of a circular cylindrical cloak. We further retrieved the wave pattern of [11], which considered an eccentric elliptic annular cloak.

To obtain general shapes, a finite Fourier expansion,

$$\rho(\theta) = a_0 + \sum_{k=1}^{n} [a_k \cos(k\theta) + b_k \sin(k\theta)], \tag{8}$$

may be used. For the sake of illustration, c.f. Fig. 2, let us consider a cloak with inner and outer boundaries expressed as

$$R_1(\theta) = 1 + 0.1\sin(\theta) - 0.15\cos(2\theta) + 0.2\sin(3\theta) + 0.1\cos(4\theta),$$

$$R_2(\theta) = 2 - 0.1\cos(2\theta) - 0.15\cos(3\theta) + 0.3\sin(3\theta) + 0.2\cos(4\theta). \tag{9}$$

It is interesting to inspect the cloak parameter values at its nonreflecting outer boundary $R_2(\theta)$. This can be done through the analysis of the entries of the inverse of the metric tensor $\mathbf{T}$ in the polar basis. We first notice in Fig. 1 that the off-diagonal terms $(T^{-1})_{r\theta}=(T^{-1})_{\theta r}$ are generally nonzero, unlike the circular case when $\mathbf{T}^{-1}$ is diagonal. Here, $\mathbf{T}^{-1}$ is diagonal only for six values of the angle θ corresponding to six points of the outer boundary where the transformed coordinate system is locally orthogonal. This demonstrates that the previous criteria for a nonreflecting interface $R_2(\theta)$, namely, $T^{-1}_{\theta\theta}=T^{-1}_{zz}=1/T^{-1}_{rr}$, $T^{-1}_{r\theta}=T^{-1}_{\theta r}=0$ (circular case [4]) and $T^{-1}_{zz}=1/T^{-1}_{rr}$ (eccentric elliptic case [11]), can be further relaxed. In general we observe that $-1<(T^{-1})_{r\theta}<1$, which reflects the rotation of the tensor $\mathbf{T}^{-1}$ with respect to its eigenbasis. Indeed, the principal refractive indices of the cloak remain positive: Along ρ we find $\sqrt{(T^{-1})_{\theta\theta}(T^{-1})_{zz}}=c_{11} \geqslant 0$ whereas along θ, $\sqrt{(T^{-1})_{rr}(T^{-1})_{zz}}=(\sqrt{c_{12}^2+f_\rho^2})/\rho' \geqslant 0$. We further note that $(T^{-1})_{rr}$ also varies with θ, unlike for circular, elliptic, and eccentric elliptic cloaks [11], and $(T^{-1})_{zz}=(T^{-1})_{\theta\theta}$ since $f_\rho=\rho'=R_2(\theta)$. Last, $0<(T^{-1})_{rr}<1$ and $(T^{-1})_{\theta\theta}>1.5$, in agreement with the fact that the cloak ought to exhibit a strong azimuthal anisotropy for the wave to be bent around it.

Let us now consider a wire source antenna centered at point $\mathbf{r}_s=(2.5,2)$. It radiates in a vacuum with wavelength $\lambda=1$ (all lengths are given in arbitrary units, micrometers for near infrared), and it carries a current $I_s=4i$. In Figs. 2 and 3, we show the wave pattern of the electric field scattered by a F-shaped lossy obstacle of permittivity $\epsilon=\epsilon_0(1+4i)$ when it is surrounded by the cylindrical cloak described above. We observe some residual interferences in Fig. 3. For a comparable mesh, interferences are less apparent in the circular and elliptic cases [8,12]; this suggests the experimental realization of an arbitrarily shaped cloak would be fairly challenging.

Last, it is interesting to compare these numerical results carried out in the intense near-field limit with those obtained from an analytical approach. For this, we compute the Green's function of Helmholtz's equation in the transformed coordinates. The electric field E_z is therefore given by $E'_z(\rho',\theta')=E_z[\rho(\rho',\theta'),\theta(\theta')]$, with $\rho(\rho',\theta')$ and $\theta(\theta')$ given by the inverse map of the map defined by Eq. (1). We used the software Mathematica to produce the corresponding ray picture (see Fig. 4). Comparing this "ideal" cloaking with that of Figs. 2 and 3, we notice that the electromagnetic eigenfield penetrates the cloak deeper than in the ray model. The singular behavior of $\mathbf{T}^{-1}$ on the inner boundary of the cloak might be incriminated.

In this Letter, we analyzed the electromagnetic response of an arbitrarily shaped cloak in presence of a closely located antenna. We compared the full-wave picture with an analytic computation of the Green's function in the transformed coordinates. We noticed the strong similarities in the numerical results, which suggests that this cloaking mechanism depends little upon whether we are in the ray optics or resonance regime. Our design can be extended straightforwardly to three-dimensional cloaks of arbitrary shape. For this, consider a transformed radial coordinate $\rho'(\rho,\theta,\phi)$ where the angle $\phi\in[0,\pi)$ replaces the longitudinal coordinate $z\in\mathbb{R}$ in Eq. (1). Then describe the inner and outer boundaries $R_1(\theta,\phi)$ and $R_2(\theta,\phi)$ of the cloak using the Fourier series.

This work has been performed in the framework of the POEM project ANR-06-NANO-008.

References

1. J. B. Pendry, Phys. Rev. Lett. **85**, 3966 (2000).
2. G. W. Milton, N. A. P. Nicorovici, R. C. McPhedran, and V. A. Podolskiy, Proc. R. Soc. London Ser. A **461**, 3999 (2005).
3. S. Guenneau, B. Gralak, and J. B. Pendry, Opt. Lett. **30**, 1204 (2005).
4. J. B. Pendry, D. Schurig, and D. R. Smith, Science **312**, 1780 (2006).
5. U. Leonhardt, Science **312**, 1777 (2006).
6. A. Alu and N. Engheta, Phys. Rev. E **95**, 016623 (2005).
7. G. W. Milton and N. A. Nicorovici, Proc. R. Soc. London Ser. A **462**, 3027 (2006).
8. F. Zolla, S. Guenneau, A. Nicolet, and J. B. Pendry, Opt. Lett. **32**, 1069 (2007).
9. D. Schurig, J. J. Mock, B. J. Justice, S. A. Cummer, J. B. Pendry, A. F. Starr, and D. R. Smith, Science **314**, 977 (2006).
10. W. Cai, U. K. Chettiar, A. V. Kildiev, and V. M. Shalaev, Nat. Photonics **1**, 224 (2007).
11. D. Kwon and D. H. Werner, Appl. Phys. Lett. **92**, 013501 (2008).
12. A. Nicolet, F. Zolla, and S. Guenneau, IEEE Trans. Magn. **44**, 1150 (2008).
13. M. Rham, D. Schurig, D. A. Roberts, S. A. Cummer, D. R. Smith, and J. B. Pendry, Photonics Nanostruct. Fundam. Appl. **6**, 87 (2008).
14. A. Nicolet, J. F. Remacle, B. Meys, A. Genon, and W. Legros, Appl. Phys. **75**, 6036 (1994).
15. P. Dular, C. Geuzaine, F. Henrotte, and W. Legros, IEEE Trans. Magn. **34**, 3395 (1998) (see also http://geuz.org/getdp/).